Filtering and Thresholding the Analytic Signal Envelope in order to improve Peak and Spike Noise Reduction in EEG Signals

Umberto Melia *, Francesc Clariá **, Montserrat Vallverdú *, Pere Caminal *

*Dept. ESAII, Centre for Biomedical Engineering Research, Universitat Politècnica de Catalunya, CIBER of Bioengineering, Biomaterials and Nanomedicine (CIBER-BBN), Barcelona, Spain; email: umberto.melia@upc.edu, montserrat.vallverdu@upc.edu, pere.caminal@upc.edu.
**Dept. IIE, Lleida University, Spain; email: claria@diei.udl.es

Total word count: 3443words

ABSTRACT
To remove peak and spike artifacts in biological time series has represented a hard challenging in the last decades. Several methods have been implemented mainly based on adaptive filtering in order to solve this problem. This work presents an algorithm for removing peak and spike artifacts based on a threshold built on the analytic signal envelope. The algorithm was tested on simulated and real EEG signals that contain peak and spike artifacts with random amplitude and frequency occurrence. The performance of the filter was compared with commonly used adaptive filters. Three indexes were used for testing the performance of the filters: Correlation coefficient (ρ), mean of coherence function (C) and rate of absolute error (RAE). All these indexes were calculated between filtered signal and original signal without noise. It was found that the new proposed filter was able to reduce the amplitude of peak and spike artifacts with $\rho > 0.85$, $C > 0.8$, $RAE < 0.5$. These values were significantly better than the performance of LMS adaptive filter ($\rho < 0.85$, $C < 0.6$, and $RAE > 1$).

Keywords: Biomedical signal processing, electroencephalography, digital filters.

1. Introduction

Electroencephalographic (EEG) signal is very susceptible to a variety of large signal contamination such as power line noise, biological or electrode artifacts. As these artifacts can be associated to cerebral activity they should be removed by filtering before further signal analysis. However, traditional methods, such as band-pass filter, are not adequate if the frequency band of the contaminant signal is within the band of the true signal, for example the electromyographic signal and the power line noise. There exist other kinds of artifacts that need different approaches to be removed, for example, certain peak and spike noise, heart electrical activity present throughout the body [1], short-time high-amplitude events in the recorded EEG for the evaluation of epileptic seizures that mask the quasi-periodic structure of the seizures [2]. The most commonly used approaches for these problems are filters mainly based on adaptive algorithms with linear and nonlinear structures [3, 4] or eigenvalue decomposition [5]. Furthermore, eye blinks and movements of the eye balls produce electrical activity along the scalp that interferes with the EEG. In order to remove ocular artifacts from EEG, many regression-based techniques have been proposed [6-11]. They require calibration trials in order to estimate the electrooculogram (EOG) component from each one of the EEG channels and then they remove it by subtraction. Independent component analysis (ICA) represents an efficient way [12, 13] to perform EOG signal separation from the EEG signals. Several methods for dealing with ocular artifacts in the EEG were reviewed by Croft et *al.* [14], focusing on the relative merits of a variety of EOG correction procedures. A noise cancellation method based on adaptive filtering was implemented by He *et al*. [15] with the aim of removing ocular artifacts from on-line EEG without calibration trials but using the EOG signal as reference. Furthermore, the acquisition of EEG during functional magnetic resonance imaging (fMRI) procedure is contaminated by numerous possible sources of artifacts, such as short-time and high-amplitude events for instance burst suppression, artifacts originated from the surrounding electromagnetic field, the fMRI-related gradient artifacts, and cardiac pulse interference [16]. These are induced effects due to alterations in the magnetic field gradient [17-20]. Artifacts induced in EEG recordings by electrical impedance tomography (EIT) are analogous to those generated by interictal spike-triggered fMRI during simultaneous EEG and fMRI monitoring. In order to remove EIT artifacts, Fabrizi *et al.* [21] used a bank of hardware filter (first-order passive high-pass filters and second-order passive low-pass filters) associated with a digital filter based on a single template of the EIT noise. A new methodology to reduce these artifacts was proposed by Melia *et al.* [22] where a filter based on the analytic signal envelope was designed. This filter can be applied to each single-channel recording without using any reference signal. In the present work, an improvement of the filter algorithm is presented, that consists in introducing a threshold calculated on the analytic signal envelope. The algorithm was tested using simulated and real EEG

signals corrupted by noise with peaks and spikes of high amplitude. Spike refers to sharp impulses of linearly rising and falling edges with a pointed peak and duration of about 80 ms. Peak refers to an isolated event with value out of the range of the signal variance.

2. Materials and Methods

2.1 The Hilbert Transform and the Analytic Signal

The Hilbert transform $\hat{x}(t)$ is a linear function of a signal $x(t)$. It is obtained from the convolution of $x(t)$ with $(\pi\ t)^{-1}$ [23, 24]. The analytic signal $y(t)$ of a real signal $x(t)$ can be written as

$$y(t) = x(t) + j\hat{x}(t) = \ m(t)\cos\big(\phi(t)\big) + j\ m(t)sin\big(\phi(t)\big) \tag{1}$$

where $x(t)$ can be expressed as the product of two signals

$$x\ (t) = m(t)\cos(\phi(t)) \tag{2}$$

Expression (2) shows that $x(t)$ can be modified in two different ways, by varying the amplitude $m(t)$ and/or by varying the phase $\phi(t)$. The simultaneous dual behavior of $x(t)$ in amplitude and frequency modulation suggests that changes in the signal amplitude leave its zero crossings unchanged. Therefore, the aim of this procedure is to modify the amplitude without altering the components that could cause the zero crossings on the time axis.

The contribution of the amplitude $B_{AM}^2$and phase B_{FM}^2 of a signal to its bandwidth [24] is defined by (3-5), where $m(t)^2 = |y(t)|^2 = y(t)\ y^*(t)$ is the instantaneous power or energy density (see Appendix).

$$B^2 = B_{AM}^2 + \ B_{FM}^2 \tag{3}$$

where B is the total bandwidth of the signal $x(t)$

$$B_{AM}^2 = \frac{1}{4\pi^2}\int\left(\frac{m(t)'}{m(t)}\right)^2 m(t)^2 dt \tag{4}$$

$$B_{FM}^2 = \int\big(f_i(t) - \ \bar{f}\big)^2 m(t)^2 dt \tag{5}$$

where $m(t)'$ is the derivative of the analytic signal envelope $m(t)$, $f_i(t) = \frac{1}{2\pi}\frac{\mathrm{d}\phi(t)}{\mathrm{d}t}$ is the instantaneous frequency function and $\bar{f}$ is the mean frequency of the spectral density of $y(t)$.

The term B_{AM}^2 associated with the analytic signal amplitude contributes to the low frequencies of B and the term B_{FM}^2 associated with the analytic signal phase contributes to the high frequencies of B. In this way, the expression B_{AM} determines the bandwidth with which $m(t)$ contributes to the signal $x(t)$ and thus it adjusts the bandwidth of a filter that applied to $m(t)$ removes the peaks and spikes from $x(t)$.

2.2 Description of the Filter Algorithm

The proposed algorithm consists of an analytic signal envelope filtering (ASEF) that reduces the amplitude of peaks or spikes in the EEG signals. Firstly, the envelope $m(t)$ of a signal $x(t)$ is filtered using a low-pass filter with a pass band B_{AM}, then a threshold $Th(t)$ based on the filtered envelope $m_{filt}(t)$ is defined and finally this threshold is applied to the envelope $m(t)$. This $Th(t)$ is calculated at each time sample of $m_{filt}(t)$ as

$$Th(t) = m_{filt}\ (t) + k\ \overline{m_{filt}} \tag{6}$$

where $\overline{m_{filt}}$ is the mean value of $m_{filt}\ (t)$ and k is an arbitrary constant.

The main steps of the proposed filter algorithm applied to a signal $x(t)$ are:

1) To calculate the analytic signal $y(t)$ of $x(t)$.

2) To calculate the envelope $m(t)$ and the instantaneous phase $\phi(t)$.
3) To filter the $m(t)$ by using a FIR filter with a cut off frequency B_{AM} in order to obtain $m_{filt}(t)$.
4) To preserve the samples that satisfy $m(t) < Th(t)$ in order to obtain the signal $m_{Th}(t)$ (7).
5) To multiply the filtered envelope $m_{Th}(t)$ by $cos\phi(t)$, in order to obtain the final filtered signal $x_{filt}(t)$ (8).

$$m_{Th}(t) = \begin{cases} m_{filt}(t): if\ m(t) \geq Th(t) \\ m(t): \quad if\ m(t) < Th(t) \end{cases} \tag{7}$$

$$x_{filt}(t) = m_{Th}(t) cos\phi(t) \tag{8}$$

This filter removes all or part of the peaks or spikes (depending on k value of $Th(t)$) in the original signal $x(t)$, preserving its frequency information.

2.3 Simulated Time Series

A set of simulated time series $x(t)$ of EEG signals corrupted by peak or spike noise was generated.

$$x(t) = s(t) + n(t) \tag{9}$$

where $s(t)$ represents the pure EEG signal and $n(t)$ a signal containing random events of peak or spike waveforms.

The signals $s(t)$ were created by using functions that generate simulated EEG data [25]. These functions create uncorrelated noise generated such that its power spectrum matches the power spectrum of human EEG. The simulated EEG was constructed by summing together a number of phase-randomized sinusoids (frequencies from 0.1 to 125 Hz and phase between 0 and 2π), the amplitude of which varied with frequency according to the power spectrum of empirical EEG data. Because this process amounts to an inverse-Fourier transform (with randomized phase) of a spectral analysis of real data, the simulated data match closely the features of empirically observed EEG data [26-27]. The mean value of $s(t)$ is $\overline{s(t)} = 0$ and the standard deviation is bounded $0.6 < \sigma_s < 1\ \mu V$.

The noise $n(t)$ was created combining peak and spike events with random amplitude and random frequency of occurrence, in order to simulate the worsts noisy case in the EEG signal. The spike events were simulated with triangle waveforms, $tri(t)$

$$tri(t) = \begin{cases} \mu_{tri}(1 - |t - t_{tri}|): & if\ 0 \leq t \leq 2t_{tri} \\ 0: & otherwise \end{cases} \tag{10}$$

where μ_{tri} is a random variable that has normal distribution with expected value $\bar{\mu}_{tri} = 0$, standard deviation $20\sigma_s$, and t_{tri} = 0.04 s. These values permitted to create triangle waveforms with negative or positive values about 20 times the maximum EEG value and with duration that simulates short-time spike EEG artifacts. Then, the signal noise $n(t)$ was built as

$$n(t) = \begin{cases} tri(t - t_{n1}): & if\ t = t_{n1} \\ \mu_{peak}: & if\ t = t_{n2} \\ 0: & otherwise \end{cases} \tag{11}$$

where μ_{peak} is a random variable that has normal distribution with expected value $\bar{\mu}_{peak}$ =0 and standard deviation $20\sigma_s$, $t_{n1} \in T_1 = \{t_{11}, t_{21}, t_{31}, \dots, t_{N1,}\}$ and $t_{n2} \in T_2 = \{t_{12}, t_{22}, t_{32}, \dots, t_{N2,}\}$, $\forall\ n = 1, 2, \dots, N$ with N = 40. Where t_{n1} and t_{n2} are random variables with normal distribution and expected value $\bar{t}_{n1} = 50$ s and standard deviation σ_{tn} = 50 s. These values permitted to create noise events, with negative or positive values about 20 times the maximum EEG value, that occur between 0 s to 100 s with Gaussian distribution.

Two sets of 1000 signals $x(t)$ were generated with a sampling frequency of 256 Hz and a length of 100 s: set EEG1, 1000 signals corrupted with isolated peak and spike noise; set EEG2, 1000 signals corrupted with isolated peak and spike noise and with 20 consecutive triangle waveforms $(tri(t))$ in two randomly selected windows of 2 s along the signal. In this way, set EEG2 contains signals more contaminated than EEG1.

2.4 Calculation of parameters B_{AM} and k of Th(t)

In order to obtain the cutoff frequency value of the low-pass filter, equation (4) was applied to each signal $s(t)$ and $x(t)$ of the set EEG2, since it represents the worst case of noise. Then, the bandwidth B_{AM} of the envelope $m(t)$ was calculated for each signal. The values of B_{AM} are shown in Fig. 1 where the mean value of B_{AM} is $\overline{B_{AM}}$= 1.895 ± 0.0514 Hz for the signals $x(t)$ and $\overline{B_{AM}}$= 0.9068± 0.1068 for the signals $s(t)$. This last value could represent the filter bandwidth value to theoretically eliminate all

peaks. In this way, a bandwidth of B_{AM} =1 Hz can be an acceptable value and it was taken into account for the present study. In the same way, the total bandwidth B was calculated from the equation (3) obtaining a mean value $\bar{B}$= 57.44± 2.86 Hz for $x(t)$ signals and $\bar{B}$= 25.19± 3.00 Hz for $s(t)$ signals.

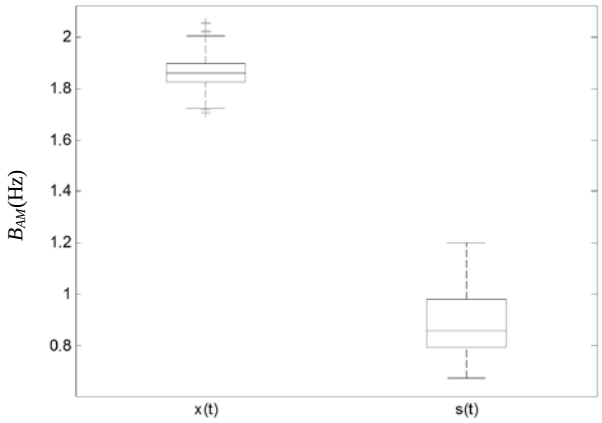

Fig.1 – Envelope bandwidth B_{AM}: signal $x(t)$ with noise ($\overline{B_{AM}}$= 1.895 ± 0.0514) and signal $s(t)$ without noise ($\overline{B_{AM}}$= 0.9068± 0.1068).

In order to find the best value of k to calculate $Th(t)$ (6) that permits to have the best performance in peak and spike removal, the ASEF algorithm was applied to the $x(t)$ signals of the set EEG2, varying k in the $0.1 \leq k \leq 1.2$ range.

For each $x_{filt}(t)$ and $s(t)$ signal, the coherence function ($C_{xs}(f)$) and an index based on the rate of the absolute error (*RAE*) before and after filtering were applied for validation.

$C_{xs}(f)$ [28] is a function of the power spectral densities (P_{xx} and P_{ss}) and the cross power spectral density (P_{xs}) of $x(t)$ (or $x_{filt}(t)$) and $s(t)$.

$$C_{xs}(f) = \frac{|P_{xs}(f)|^2}{P_{xx}(f)P_{ss}(f)} \tag{12}$$

where $0 \leq C_{xs}(f) \leq 1 \; \forall f$. The function $C_{xs}(f)$ indicates how well the signal $x(t)$ (or $x_{filt}(t)$) corresponds to $s(t)$ at each frequency f. In this work, the index C was defined as the mean value of $C_{xs}(f)$ with respect to f.

The index *RAE* was defined as

$$RAE = \frac{E\left[\left|s(t) - x_{filt}(t)\right|\right]}{E[|s(t) - x(t)|]} \tag{13}$$

In this way, low values of *RAE* denote low absolute error after filtering, indicating good efficiency in the removal of peak and spike noise $n(t)$.

The optimum k_b value was defined as the average of those k values corresponding to the minimum *RAE* and the maximum C. For the set EEG2, k_b = 0.43±0.07 is the optimum value (as seen in Fig. 2) and this is the value of k that will be taken into account in the present study.

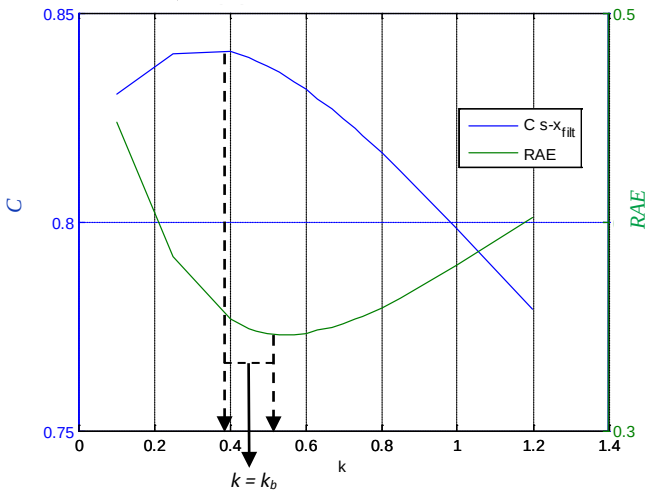

Fig.2 – Mean value of *RAE* and *C* with respect to *k* for all $x(t)$ signals of EEG2 set. The obtained *k* value is $k = k_b$=0.43.

2.5 Performance Test

In order to test the performances of the proposed ASEF algorithm and compare it with other filters [29-31], several known filters were applied to each simulated signal $x(t)$ for obtaining a set of filtered signals $x_{filt}(t)$. These selected filters are:

- FIR (Finite Impulse Response) filter of 200th-order with a bandwidth of 0.1-30 Hz, since the calculated *B* value of $s(t)$ signals is $\bar{B}$= 25.19± 3.00.
- LMS (Least Mean Square) adaptive filter of 500th-order with step size of 0.0001, using $s(t)$ as reference signal.
- NLMS (Normalized Least Mean Square) adaptive filter of 300th-order with step size of 0.1, no leakage and using $s(t)$ as reference signal.
- RLS (Recursive Least Square) adaptive filter of 100th-order, using $s(t)$ as reference signal.

All parameters of the adaptive filters were chosen after several tests on a subset of simulated EEG data randomly chosen, in order to provide the highest correlation coefficient (ρ) and C and the lowest RAE, to guarantee filter stability with a reasonable computational cost.

The performances of ASEF filtering were evaluated using:

- ASEF without using the threshold $Th(t)$ [22].
- ASEF using the threshold $Th(t)$ with k=0.43.

In order to evaluate the performance of each filter, the correlation coefficient (ρ), *C* and *RAE* were calculated between signal $x_{filt}(t)$ and $s(t)$.

2.6 Real EEG Data

Finally, ASEF was tested on real EEG data ($s(t)$ signal). Noise signal $n(t)$ was added to each signal $s(t)$ and then the ASEF was applied to the corrupted signal $x(t)$ (9).

The recordings $s(t)$ belong to the EEG database that are available online by Andrzejak et al (2001) at the Department of Epileptology, University of Bonn (Germany) [32]. For the evaluation, two different subsets (A, B) were used, which contain surface EEG signals recorded from five healthy volunteers who were relaxed in the awaking state. Whereas the subjects had their eyes open during the recording of the EEG in subset A, the EEG signals of subset B were acquired with eyes closed. Each subset contains 100 single-channel EEG signals of 23.6 s, recorded with a sampling frequency of 173.6 Hz (4096 sample points).

3. Results

3.1 Simulated Time Series

The ASEF filtering reduces the amplitude of the peak and the triangular waveforms $n(t)$ without changing in a significant way the components of the pure signal $s(t)$. This effect can be observed in Fig. 3a where ASEF filtering was applied to a simulated corrupted signal $x(t)$. A segment of 5 seconds of the signal $x(t)$ and its corresponding filtered signal $x_{filt}(t)$ are shown in in Fig. 3b. In a similar way, Fig. 3c presents the same five-second segment of the $x(t)$ signal and its corresponding filtered signal $x_{filt}(t)$ by an adaptive filter LMS. Comparing Fig. 3b and Fig. 3c, it can be observed that ASEF filtering (Fig. 3b) and the adaptive filter (Fig. 3c) both present a reduction of the noise $n(t)$, but ASEF does not present any distortion of the $s(t)$ signal such as adaptive filter does.

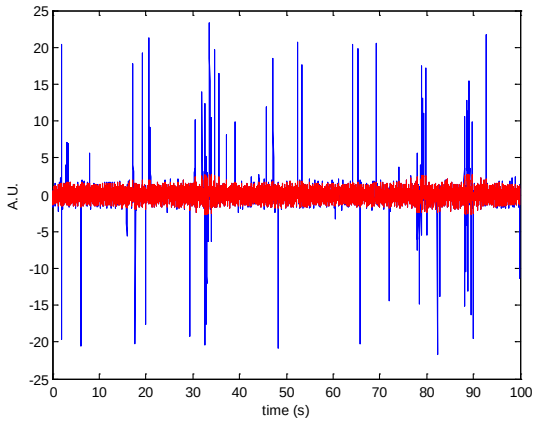

(a)

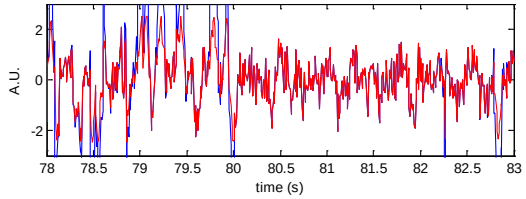

(b)

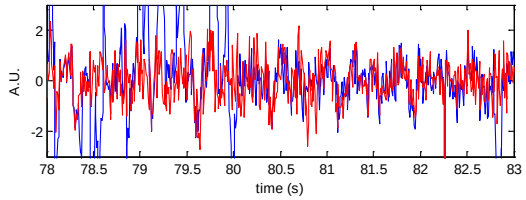

(c)

Fig. 3. (a) A simulated signal $x(t)$ with peaks and its filtered signal $x_{filt}(t)$ with ASEF filtering using the threshold $Th(t)$ with $k = 0.43$. (b) Zoom of 5 second segment of the $x(t)$ and $x_{filt}(t)$ signals. In red $x_{filt}(t)$, and in blue $x(t)$. (c) Zoom of 5 second segment of $x(t)$ and $x_{filt}(t)$ signals filtered with an adaptive filter LMS. In red $x_{filt}(t)$, and in blue $x(t)$.

Table 1 shows that the value of ρ between $s(t)$ and $x_{filt}(t)$ was in the range of $0.5<\rho<0.85$ for the adaptive filters and the ASEF filtering without $Th(t)$. However, only the ASEF filtering with $Th(t)$ could obtain $\rho > 0.85$.

Table 1. Evaluation Performance: Pearson Correlation Coefficient (ρ)

Filter	EEG1 (m±σ)
ASEF TH k=0.43	0.9085 ±0.0149
ASEF no TH	0.8283±0.0182
FIR	0.3839±0.0853
LMS	0.8075±0.0578
NLMS	0.7629±0.0643
RLS	0.5366±0.1562

m, mean; σ, standard deviation

Fig. 4 presents the boxplot of the C and *RAE* values calculated for all signals of EEG1 sets, in order to compare the performance of all filters. As it can be noted, ASEF filtering with $Th(t)$ gives the best values of the *RAE* and the C.

The performance of the ASEF without $Th(t)$ was quite similar to the adaptive filters in terms of *RAE* but present higher value of C. Considering the performance of the best adaptive filter (LMS), it can be noted that even if the peak noise $n(t)$ is reduced, the filtering affects also the pure signal $s(t)$ and consequently *RAE* is higher in LMS than in ASEF and C is lower in LMS than in ASEF.

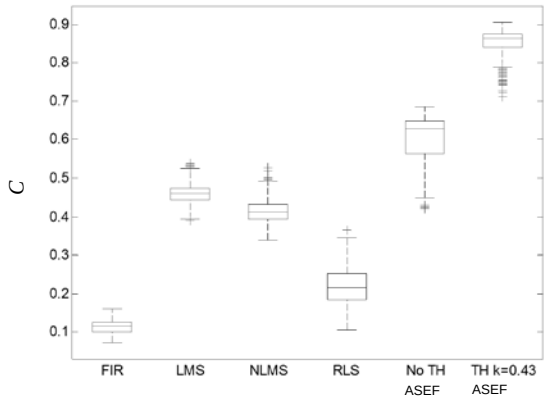

(a)

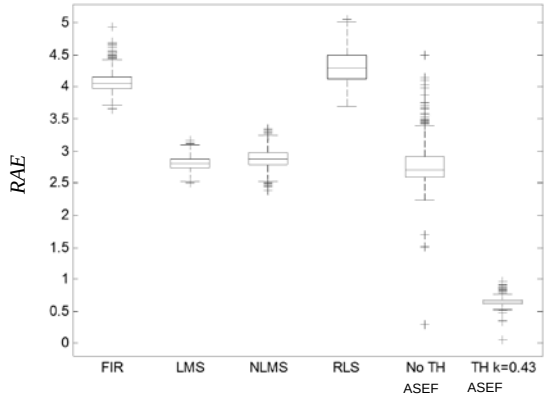

(b)

Fig. 4. (a) Distribution of C values and (b) distribution of *RAE* values calculated for all simulated signals $x(t)$ of the EEG1 set. On each box, the central mark is the median, the edges of the box are the 25th and 75th percentiles. The whiskers are lines extending from each end of the boxes to show the extent of the rest of the data. Values beyond the end of the whiskers are considered outliers and marked with a +.

3.2 Real EEG data

Fig. 5a shows an example of an EEG signal before and after ASEF filtering with $Th(t)$. The effect of the filtering was tested by calculating the indexes *RAE* and C on unfiltered EEG, on EEG filtered with ASEF (without and with $Th(t)$) and on adaptive filter (LMS). The LMS adaptive filter was chosen because it gave better performance than all other adaptive filters when applied to the simulated dataset (as seen in Fig. 4). The results of *RAE* and C indexes calculated from $s(t)$ and $x_{filt}(t)$ are presented in Fig. 5b and Fig. 5c. It can be observed a quite low value of *RAE* and high value of C when ASEF is applied with k=0.43. Also, it can be noted that *RAE* of LMS and ASEF without $Th(t)$ get values higher than the unit, that corresponds to non-filtered EEG ($x(t) = x_{filt}(t)$). This means that filtering with these procedures introduces other type of noise to the original signal $s(t)$, consequently, the absolute error value in the signal $x_{filt}(t)$ is higher than in the signal $x(t)$. The obtained values of ρ between $s(t)$ and $x_{filt}(t)$ were similar to those of simulated data: $0.55<\rho<0.85$ for the LMS and the ASEF filtering without $Th(t)$ and $\rho > 0.85$ for ASEF filtering with threshold $Th(t)$.

These results denote a good performance in the removal of peaks and spikes also in real EEG data as well as in simulated EEG data.

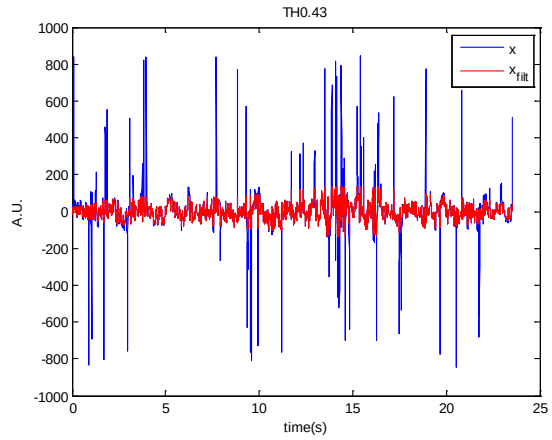

(a)

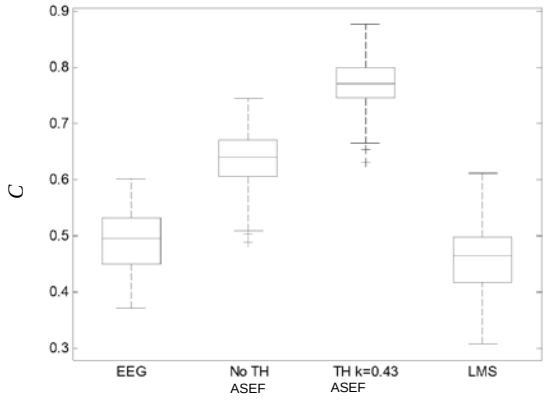

(b)

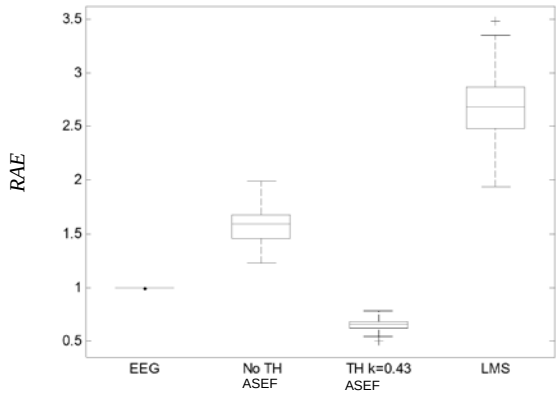

(c)

Fig. 5. (a) $x(t)$ is a real EEG signal $s(t)$ with peaks $n(t)$ and $x_{filt}(t)$ is the filtered signal by using ASEF. (b) Distribution of C values and (c) distribution of *RAE* values calculated between $x(t)$ and the filtered $x_{filt}(t)$ in a set of 200 real EEG signals. EEG box represents the index calculated taken $x(t)$ instead of $x_{filt}(t)$. On each box, the central mark is the median, the edges of the box are the 25th and 75th percentiles. The whiskers are lines extending from each end of the boxes to show the extent of the rest of the data. Values beyond the end of the whiskers are considered outliers and marked with a +.

3.3 Uncorrupted signals

Finally, the algorithm was applied to signals without any contamination. Table 2 shows C, *RAE* and ρ values obtained applying *ASEF* with k=0.43 to all signals $s(t)$ without any contamination, belonging to EEG1 set and real EEG data. In order to avoid division by zero in *RAE* calculation since $x(t)=s(t)$, the denominator of the (13) was calculated using $x(t)=\overline{s(t)}$ where $\overline{s(t)}$ is the

mean value of $s(t)$. Observing the values of Table 2 (C >0.95, *RAE*<0.25 and ρ > 0.98), it can be deduced that the *ASEF* with k=0.43 does not modify uncontaminated signals inappropriately.

Table 2. Evaluation Performance: C, *RAE* and Pearson Correlation Coefficient (ρ) for *ASEF* with k=0.43 applied to signals $s(t)$

Index	EEG1 (m±σ)	real EEG (m±σ)
C	0.9561±0.0081	0.9721±0.0145
RAE	0.0659±0.0107	0.0568±0.0236
ρ	0.9883±0.0025	0.9889±0.0056

m, mean; σ, standard deviation

4. Conclusions and Discussions

An algorithm for removing peak and spike noise from EEG is presented in this paper. This is based on filtering and thresholding the analytic signal envelope. This filter preserves all information contained in the original signal phase, changing only the bandwidth of the envelope. It was tested on a set of simulated and real EEG signals corrupted with peak and spike noise $n(t)$ and its performance was compared with adaptive filters calculating correlation coefficient (ρ), mean of coherence function (C) and rate of absolute error (*RAE*).

Firstly, the optimum bandwidth B_{AM} = 1 Hz of the envelope of a signal without peaks was calculated. Then applying C and *RAE* indexes, the optimum value of the parameter k of the threshold $Th(t)$ was calculated on a subset of simulated EEG signals, obtaining k=0.43. Finally, using these values of k and B_{AM}, the ASEF was applied on a dataset of simulated and real EEG signals both corrupted with noise $n(t)$.

It can be noted from table 1 and Fig. 4 that ASEF with k= 0.43 has the highest ρ and C for both EEG1 and EEG2 sets; this demonstrates the capability of the filter to retain the shape of the signal and also to preserve its frequency content. These values are even higher than the ρ and C of the best adaptive filter which was LMS filter. Furthermore, ASEF with k= 0.43 has the lowest value of *RAE*. This means that ASEF with k= 0.43 has the best performance in reducing the noise without changing the original signal for all the time of recording. The optimization of B_{AM} and k values will permit to preserve the episodes of consecutive spikes with physiological information.

The results of the simulated signals were validated applying the ASEF algorithm to real EEG data corrupted by noise $n(t)$, obtaining analogous performance results that simulated data. It has been demonstrated that this filter presents better performance than adaptive filters applied to signals corrupted by non-periodic peak and spike noise. A remarkable feature of this filter is that once the value of the parameters B_{AM} and k are obtained, for one kind of signal, it is not necessary to recalculate these parameters for future filtering of the same physiological signal. The parameters B_{AM} and k calculated in this study have represented efficient values for EEG signal, however different values of B_{AM} and k will permit to adapt the filter to the features of the different physiological signals and noise situations.

The main aspect of the ASEF is that the amplitude of the signal $x(t)$ is modified without changing the phase $\phi(t)$ using only the filtered envelope $m_{filt}(t)$. The filtered signal $x_{filt}(t)$ presents a reduction of the peak and spike amplitude compared with the original signal $s(t)$ (*RAE*<0.5), but without affecting the frequency components (C >0.8). It should be noted that all this can be calculated in the time domain without needing any reference signal or any multichannel recording. This is advantageous when it is necessary to minimize the number of channels in a recording.

The concept and the methodology of this filter is similar to our previous designed filter published in [22], but in this current paper the algorithm for the calculation of the bandwidth of the envelope at low frequencies of the generic signal was improved and a threshold based on the filtered envelope was introduced. These modifications have permitted to improve the performance in terms of C, *RAE* and Pearson Correlation Coefficient (ρ). This new designed filter minimizes the inappropriate modification of the original signal $s(t)$.The results have shown the capability of ASEF in reducing the noise, minimizing the absolute error rate between filtered and pure signal in both simulated and real EEG data.

Appendix

The standard deviation σ_f, commonly known as bandwidth B, is defined as

$$B^2 = {\sigma_f}^2 = \int (f - \bar{f})^2 |Y(f)|^2 \, df = \overline{f^2} - \bar{f}^2 \tag{14}$$

where the spectral density $|Y(f)|^2$ is the Fourier transform of the autocorrelation function of the signal $y(t)$.

The time expression for the mean frequency can be calculated as

$$\bar{f} = \int f \, |Y(f)|^2 \, df = \frac{1}{j2\pi} \int j2\pi f \, Y(f) Y^*(f) df = \frac{1}{2\pi} \int y^*(t) \frac{1}{j} \frac{dy(t)}{dt} dt \tag{15}$$

More specifically, if $y(t) = m(t)\, e^{j\phi(t)}$ then

$$\bar{f} = \frac{1}{2\pi} \int y^*(t) \frac{1}{j} \frac{dy(t)}{dt} dt = \frac{1}{2\pi} \int \frac{d\phi(t)}{dt} m(t)^2\, dt \tag{16}$$

In similar way, the time expression of the mean square frequency is deduced as

$$\overline{f^2} = \int f^2\, |Y(f)|^2\, df = \frac{1}{(j2\pi)^2} \int j2\pi f\ \ Y(f)\ \ j2\pi f\ \ Y^*(f) df = \frac{1}{4\pi^2} \int \left| \frac{dy(t)}{dt} \right|^2 dt \tag{17}$$

Then, the mean square frequency value for $y(t) = m(t)\, e^{j\phi(t)}$ is

$$\overline{f^2} = \frac{1}{4\pi^2} \int \left| \frac{dy(t)}{dt} \right|^2 dt = \frac{1}{4\pi^2} \int \left(\frac{dm(t)}{dt} \right)^2 dt + \frac{1}{4\pi^2} \int \left(\frac{d\phi(t)}{dt} \right)^2 m(t)^2 dt \tag{18}$$

Finally, from the square of the signal bandwidth (14) in Hz and from the instantaneous frequency definition $f_i = \frac{1}{2\pi} \frac{d\phi(t)}{dt}$, the following expression is obtained

$$B^2 = \frac{1}{4\pi^2} \int \left(\frac{m(t)'}{m(t)} \right)^2 m(t)^2 dt + \int \left(f_i(t) - \bar{f} \right)^2 m(t)^2 dt \tag{19}$$

Consequently, the square bandwidth is made by a term that depends on the mean of the amplitude and another term that depends on the mean of the frequency $B^2 = B_{AM}^2 + B_{FM}^2$.

Acknowledgment

This work was supported within the framework of the CICYT grant TEC2010-20886 from the Spanish Government and the Research Fellowship Grant FPU AP2009-0858 from the Spanish Government. CIBER of Bioengineering, Biomaterials and Nanomedicine is an initiative of ISCIII.

Author Declaration

Competing interests: None declared
Funding:None
Ethical approval: Not required

References

[1] Witte H, Glaser S, Rother M, New spectral detection and elimination test algorithms of ECG and EOG artefacts in neonatal EEG recordings. Med. Biol. Eng. Comput. 1987; 25: 127-130.
[2] Celka P, Boashash B, Colditz P, Preprosessing and time-frequency analysis of newborn EEG seizures. IEEE Eng. Med. Biol. Mag. 2001; 20: 30–39.
[3] Haykin S, Adaptive Filter Theory. 3th Ed. Upper Saddle River: Prentice-Hall;1996.
[4] Lim SJ, Harris JG, Combined LMS/F algorithm. Electr. Lett. 1997; 33: 467-468.
[5] Hajipour S, Shamsollahi MB, Albera L, Merlet I, Noise cancelation of epileptic interictal EEG data based on generalized eigenvalue decomposition. 35th International Conference on Telecommunications and Signal Processing (TSP) , 3-4 July 2012, pp. 591-595.
[6] Verleger R, Gasser T, Mocks J, Correction of EOG artifacts in event-related potentials of the EEG: Aspects of reliability and validity. Psychophysiology 1982; 19: 472-480.
[7] Gratton G, Coles MGH, Donchin E, A new method for off-line removal of ocular artifacts. Electroenceph. Clin. Neurophysiol. 1983; 55: 468-484.
[8] Kenemans JL, Molenaar ECM, Verbaten MN, Slangen JL, Removal of the ocular artifact from the EEG: A comparison of time and frequency domain methods with simulated and real data. Psychophysiology 1991; 28: 115-121.
[9] Whitton JL, Lug E, Moldofsky H, A spectral method for removing eye movement artifacts from the EEG. Electroenceph. Clin. Neurophysiol. 1978; 44: 735-741.
[10] Woestenburg JC, Verbaten MN, Slanger JL, The removal of the eye-movement artifact from the EEG by regression analysis in the frequency domain. Biological Psychology 1983; 16: 127-147.
[11] Veneri G, Federighi P, Rosini F, Federico A, Rufa A, Spike removal through multiscale wavelet and entropy analysis of ocular motor noise: A case study in patients with cerebellar disease. Journal of Neuroscience Methods, 2011;196(2): 318-326.
[12] Jung TR, Makeig S, Westerfield M, Townsend J, Courchesne E, Sejnows TJ, Removal of eye activity artifacts from visual event-related potential in normal and clinical subjects. Clin. Neurophysiol. 2000; 111: 1745-1758.

[13] LeVan P, Urrestarrazu E, Gotman J, A system for automatic artifact removal in ictal scalp EEG based on independent component analysis and Bayesian classification. Clinical Neurophysiology 2006; 117(4): 912- 927.

[14] Croft RJ, Barry RJ, Removal of ocular artifact from the EEG: a review. Clinical Neurophysiology 2000; 30(1): 5–19.

[15] He PI, Wilson G, Russell C, Removal of ocular artifacts from electro-encephalogram by adaptive filtering Med. Biol. Eng. Comput. 2004; 42: 407-412.

[16] Allen PJ, Josephs O, Turner R, A method for removing imaging artifact from continuous EEG recorded during functional MRI. NeuroImage 2000; 12: 230–39.

[17] Huang C, Ju M, Lin C, A robust algorithm for removing artifacts in EEG recorded during FMRI/EEG study. Computers in Biology and Medicine, 2012;42(4): 458-467.

[18] Allen PJ, Polizzi G, Krakow K, Fish DR, Lemieux L, Identification of EEG events in the MR scanner: the problem of pulse artifact and a method for its subtraction. Neuroimage 1998; 8: 229–39.

[19] Garreffa G, Real-time MR artifacts filtering during continuous EEG/fMRI acquisition. Magn. Reson. Imaging, 2003; 21: 1175–89.

[20] Sijbers J, Michiels I, Verhoye M, Van Audekerke J, Van der LA, Van Dyck D, Restoration of MR-induced artifacts in simultaneously recorded MR/EEG data. Magn. Reson. Imaging 1999; 17: 1383–91.

[21] Fabrizi L, Yerworth R, McEwan A, Gilad O, Bayford R, Holder DS, A method for removing artifacts from continuous EEG recordings during functional electrical impedance tomography for the detection of epileptic seizures. Physiol. Meas. 2010; 31: S57–S72.

[22] Melia USP, Claria F, Vallverdu M, Caminal P, Removal of Peak and Spike Noise in EEG Signals Based on the Analytic Signal Magnitude. Proceedings of 34th Annual International Conference of the IEEE Engineering in Medicine and Biology Society (EMBS) 2012; 3523-3526.

[23] Marple L, Computing the discrete-time "analytic" signal via FFT. IEEE Transactions on Signal Processing 1999; 47: 2600-2603.

[24] Cohen L, Time-frequency analysis. Prentice Hall Signal Processing Series; 1995.

[25] Yeung N, Bogacz R, Holroyd CB, Nieuwenhuis S, Cohen JD, Generation of simulated EEG data. Available from: http://www.cs.bris.ac.uk/~rafal/phasereset/

[26] Yeung N, Bogacz R, Holroyd CB, Cohen JD, Detection of synchronized oscillations in the electroencephalogram: An evaluation of methods. Psychophysiology 2004; 41: 822-832.

[27] Yeung N, Bogacz R, Holroyd CB, Nieuwenhuis S, Cohen JD, Theta phase-resetting and the error-related negativity. Psychophysiology 2007; 44: 39-49.

[28] Stoica P, Moses R, Introduction to spectral analysis. Upper Saddle River; Prentice-Hall; 2005 pp.67-68.

[29] Farhang-Boroujeny B, Adaptive filters: Theory and applications. Chichester England: John Wiley & Sons; 1998.

[30] Proakis JG, Digital communications. 4th Ed. New York: McGraw-Hill; 2001.

[31] Shynk JJ, Frequency-domain and multirate adaptive filtering. IEEE Signal Processing Magazine 1992;9(1): 14-37.

[32] Andrzejak RG, Lehnertz K, Rieke C, Mormann F, David P, Elger CE, Indications of non-linear deterministic and finite dimensional structures in time series of brain electrical activity: Dependence on recording region and brain state. Phys. Rev. E 2001; 64: 0619071–0619078.